Molecular Pharmacology Fast Forward. Published on December 5, 2022 as DOI: 10.1124/molpharm.122.000597
This article has not been copyedited and formatted. The final version may differ from this version.

The glycosylated *N*-terminal domain of MUC1 is involved in chemoresistance by modulating drug permeation across the plasma membrane

Kaori Miyazaki [1], Hisanao Kishimoto [1], Hanai Kobayashi, Ayaka Suzuki, Kei Higuchi, Yoshiyuki Shirasaka, and Katsuhisa Inoue

Department of Biopharmaceutics, School of Pharmacy, Tokyo University of Pharmacy and Life Sciences (K.M., H.K., H.K., A.S., K.H., and K.I.)

Faculty of Pharmacy, Institute of Medical, Pharmaceutical and Health Sciences, Kanazawa University (Y.S.)

Molecular Pharmacology Fast Forward. Published on December 5, 2022 as DOI: 10.1124/molpharm.122.000597
This article has not been copyedited and formatted. The final version may differ from this version.

Running title: Extracellular domain of MUC1 prevents drug permeation

Corresponding author: Katsuhisa Inoue, 1432-1 Horinouchi, Hachioji, Tokyo 192-0392, Japan

Tel. & Fax: +81-42-676-3126; E-mail: kinoue@toyaku.ac.jp

Number of text pages： 26

Number of tables： 1

Number of figures：4

Number of references：43

Number of words in the Abstract: 239

Number of words in the Introduction: 651

Number of words in the Discussion: 1156

Abbreviations used:

BCRP, breast cancer resistance protein; CDDP, cisplatin; CT, cytoplasmic tail; DMSO, dimethyl sulfoxide; DOX, doxorubicin; EGF, epidermal growth factor; EGFP, enhanced green fluorescent protein; FADD, Fas-associated death domain; FD-4, fluorescein isothiocyanate-dextran 4000; 5-FU, 5-fluorouracil; GFP, green fluorescent protein; LC-MSMS, liquid chromatography-tandem mass spectrometry; MUC1, mucin 1; MUC13, mucin 13; MRP, multidrug resistance-associated protein; NG, *N*-terminal glycosylated domain; N.S., not significant; P-gp, P-glycoprotein; PNA, peanut agglutinin; PAC, paclitaxel; UEA I, ulex europaeus agglutinin I; UPLC, ultra-performance liquid chromatography; UWL, unstirred water layer

Molecular Pharmacology Fast Forward. Published on December 5, 2022 as DOI: 10.1124/molpharm.122.000597
This article has not been copyedited and formatted. The final version may differ from this version.

ABSTRACT

Mucin 1 (MUC1) is aberrantly expressed in various cancers and implicated in cancer progression and chemoresistance. Although the *C*-terminal cytoplasmic tail of MUC1 is involved in signal transduction, promoting chemoresistance, the role of the extracellular MUC1 domain (NG-MUC1) remains unclear. In this study, we generated stable MCF7 cell lines expressing MUC1 and MUC1ΔCT (cytoplasmic tail-deficient MUC1), and show that NG-MUC1 is involved in drug resistance by modulating the transmembrane permeation of various compounds without cytoplasmic tail signaling. Heterologous expression of MUC1ΔCT increased cell survival in treating anticancer drugs (such as 5-fluorouracil, cisplatin, doxorubicin, and paclitaxel), in particular by causing an approximately 150-fold increase in the IC_{50} of paclitaxel, a lipophilic drug, compared to the control [5-fluorouracil (7-fold), cisplatin (3-fold), and doxorubicin (18-fold)]. The uptake studies revealed that accumulations of paclitaxel and Hoechst 33342, a membrane-permeable nuclear staining dye, were reduced to 51% and 45%, respectively, in cells expressing MUC1ΔCT via ABCB1/P-gp-independent mechanisms. Such alterations in chemoresistance and cellular accumulation were not observed in MUC13-expressing cells. Furthermore, we found that MUC1 and MUC1ΔCT increased the cell-adhered water volume by 2.6- and 2.7-folds, respectively, suggesting the presence of a water layer on the cell surface created by NG-MUC1. Taken together, these results suggest that NG-MUC1 acts as a hydrophilic barrier element against anticancer drugs and contributes to chemoresistance by limiting the membrane permeation of lipophilic drugs. Our findings could help better understanding the molecular basis of drug resistance in cancer chemotherapy.

SIGNIFICANCE STATEMENT

Membrane-bound mucin, MUC1, aberrantly expressed in various cancers, is implicated in cancer progression and chemoresistance. Although the MUC1 cytoplasmic tail is involved in proliferation-promoting signal transduction thereby leading to chemoresistance, the significance of the extracellular domain remains unclear. Here, we clarified the role of the glycosylated extracellular

Molecular Pharmacology Fast Forward. Published on December 5, 2022 as DOI: 10.1124/molpharm.122.000597
This article has not been copyedited and formatted. The final version may differ from this version.

domain as a hydrophilic barrier element to limit the cellular uptake of lipophilic anticancer drugs. Our findings could help better understanding the molecular basis of MUC1 and drug resistance in cancer chemotherapy.

INTRODUCTION

The development of chemoresistance is a critical problem in cancer chemotherapy. Despite the current progress of radiotherapy and immunotherapy, cancer chemotherapy remains the primary option for the treatment of patients with unresectable tumors (Holohan *et al.*, 2013; Tyner *et al.*, 2022). Chemoresistance could be either inherent due to genetic characteristics or acquired due to exposure to anticancer drugs. In the latter case, multidrug resistance causes a serious problem in chemotherapy, as cancer cells become resistant to structurally and functionally unrelated drugs upon single drug treatment (Wang *et al.*, 2010; Tyner *et al.*, 2022). The underlying mechanisms of multidrug resistance involve increased drug efflux (Tyner *et al.*, 2022), activation of drug metabolism (Meijer *et al.*, 1992), drug target mutation (Kobayashi *et al.*, 2009; Adashek *et al.*, 2021), DNA damage repair (Furuta *et al.*, 2002; Zimmermann *et al.*, 2022), and inhibition of apoptosis (Montero and Haq, 2022). It is well-known that ATP-driven efflux transporters, such as ABCB1/P-gp, ABCG2/BCRP, and ABCCs/MRPs, are clinically relevant to multidrug resistance by reducing the intracellular accumulation of anticancer drugs (Tyner *et al.*, 2022). Therefore, membrane transport and the subsequent accumulation of anticancer drugs in cancer cells are suggested to be pivotal for successful cancer chemotherapy.

Mucin 1 (MUC1), a membrane-bound glycoprotein of the mucin family, is implicated in cancer progression, metastasis, and chemoresistance (Kufe, 2009; Jonckheere *et al.*, 2014). MUC1 is expressed specifically in normal epithelia including gastrointestinal tract, respiratory tract, and ocular surface, but aberrantly expressed in various types of cancers (Linden *et al.*, 2008; Kufe, 2012). MUC1 is composed of an *N*-terminal extracellular domain that is heavily *O*-glycosylated with long and

Molecular Pharmacology Fast Forward. Published on December 5, 2022 as DOI: 10.1124/molpharm.122.000597
This article has not been copyedited and formatted. The final version may differ from this version.

branched oligosaccharides (NG-MUC1), a single transmembrane domain (TM), and a *C*-terminal cytoplasmic tail (MUC1-CT). MUC1 undergoes post-transcriptional modification through autoproteolytic cleavage at a SEA domain to generate two subunits (NG-MUC1 and TM/MUC1-CT) and forms a heterodimer at the cell membrane (Levitin *et al.*, 2005; Kufe, 2012). Under inflammation and other stress conditions, MUC1 is cleaved by proteolytic enzymes and resulting in shedding of NG-MUC1 into the extracellular space and activation of MUC1-CT for intracellular signal transduction (Levitin *et al.*, 2005; Kufe, 2012). Cumulative studies have demonstrated that MUC1-CT is involved in proliferation-promoting signal transduction (Ren *et al.*, 2006; Carson, 2008; Hata *et al*, 2019). The transcription factor-associated MUC1-CT fragment localizes to the nucleus to regulate p53-mediated transcription, interacts with FADD to inhibit the binding of caspase-8 to FADD, or binds to c-Abl in the cytoplasm, and thereby controls gene expression related to epithelial-mesenchymal transition, epigenetic reprogramming, and anti-apoptotic signaling, regulated by various factors, such as p53, FADD, and c-Abl, leading to chemoresistance in cancer chemotherapy (Ren *et al.*, 2004; Wei *et al.*, 2007; Yin *et al.*, 2010).

In contrast to the well-described significance of MUC1-CT in chemoresistance, the role of NG-MUC1 remains unclear. A previous study showed that the chemical inhibition of *O*-glycosylation resulted in reduced MUC1 protein expression and increased 5-fluorouracil (5-FU) incorporation into the genomic DNA in a human pancreatic ductal adenocarcinoma cell line, suggesting that *O*-glycosylation affects MUC1 functions, thereby leading the change in 5-FU incorporation into DNA (Kalra and Campbell, 2007, 2009). Based solely on this observation, membrane-bound mucins have been thought as a physical barrier that prevents the entry of not only macromolecules but also chemicals (Leal *et al.*, 2017). However, the role of MUC1 on 5-FU sensitivity is obscure due to the presence of MUC1-CT signaling, which affects the metabolism and apoptotic effect of 5-FU. Particularly, *O*-glycosylation of NG-MUC1 might be involved in 5-FU accessibility, but the enzymatic inhibitions also suppress the surface expression of MUC1 (Leteurtre *et al.*, 2003). Furthermore, no data is available on the interaction between NG-MUC1 and organic chemicals (low-molecular weight compounds), except for

Molecular Pharmacology Fast Forward. Published on December 5, 2022 as DOI: 10.1124/molpharm.122.000597
This article has not been copyedited and formatted. The final version may differ from this version.

macromolecules such as polymers and particles (Jonckheere *et al.*, 2014). In this study, we explored the role of membrane-bound NG-MUC1 in cancer chemotherapy through the evaluation of cytotoxicity and the membrane permeation of anticancer drugs in cell lines highly expressing MUC1-ΔCT.

MATERIALS AND METHODS

Materials

Paclitaxel (PAC) was obtained from Tokyo Chemical Industry Co., Ltd. (Tokyo, Japan). Cisplatin (CDDP), doxorubicin (DOX), 5-fluorouracil (5-FU), and rose bengal were obtained from FUJIFILM Wako Pure Chemical Corporation (Osaka, Japan). Fluorescein isothiocyanate-dextran 4,000 (FD-4) was purchased from Sigma-Aldrich Co. Ltd. (St. Louis, MO). All other reagents were of analytical grade.

Cell culture

MCF7, HeLa, and HEK293 cells (RIKEN Cell Bank, Tsukuba, Japan) were grown at 37°C and 5% CO_2 in Dulbecco's modified Eagle medium (DMEM) supplemented with 100 units/ml of penicillin, 100 μg/ml of streptomycin, and 10% of fetal bovine serum (FBS). A549 cells (RIKEN Cell Bank) were grown at 37°C and 5% CO_2 in RPMI-1640 medium supplemented with 100 units/ml of penicillin, 100 μg/ml of streptomycin, and 10% of FBS. Cell lines were tested for mycoplasma contamination by DNA staining with Hoechst 33342.

Construction of plasmids

The cDNA sequences of the following accession numbers: human MUC1 (J05582) and human MUC13 (NM_033049) were obtained from GenBank™. MUC1/pcDNA3.1(+) was kindly provided by Dr. Akinori Hisatsune (University of Kumamoto, Japan) (Hisatsune *et al.*, 2009). To construct MUC1ΔCT-GFP, the coding region of the cytoplasmic tail (72 amino acid residues) of MUC1 was

Molecular Pharmacology Fast Forward. Published on December 5, 2022 as DOI: 10.1124/molpharm.122.000597
This article has not been copyedited and formatted. The final version may differ from this version.

deleted from the MUC1 cDNA, and the resulting fragment was subcloned into a pEGFP-N3 vector (Takara Bio Inc. Tokyo, Japan) in frame with EGFP. The MUC13 cDNA sequence without a stop codon was designed with synonymous codons to exclude repetitive and homologous sequences and to reduce the GC-content (below 65%), and then synthesized by Eurofins Genomics K.K. (Tokyo, Japan). The MUC13 cDNA was subcloned into a pEGFP-N3 vector in frame with the EGFP. The plasmids were isolated using Wizard™ Plus SV Minipreps DNA Purification Systems (Promega, Madison, WI). The DNA sequences of all plasmids constructed in this study were confirmed by an automated sequencer (ABI PRISM 3130, Applied Biosystems, Foster City, CA).

Transfection

For the preparation of MCF7 cells transiently expressing human MUC1, MCF7 cells (2.0×10^5 cells/well) were cultured on 24-well plates over 12 h, and transfected with 1 μg/well of MUC1/pcDNA3.1(+) plasmid by using 2 μg/well of polyethylenimine (PEI) MAX (Mw 40,000; Polysciences, Inc., PA) as a transfection reagent. Mock cells were prepared by the same transient transfection method, using an empty pcDNA3.1(+) vector. To generate cell lines stably expressing GFP-tagged human MUC1ΔCT, MCF7, HeLa, A549, and HEK293 cells were transfected with the plasmid by using PEI MAX and selected by 800 μg/mL G418 (Sigma-Aldrich Co. Ltd). The expression of GFP-tagged human MUC1ΔCT in antibiotic-resistant clones was confirmed by the observation of GFP-derived fluorescence. MCF7 cells stably expressing GFP-tagged human MUC1 or MUC13 were prepared and selected similarly. Each mock cells corresponding to the original cell line were prepared by the same transfection method with an empty pcDNA3.1(+) vector owing to G418-resistance same as that of the pEGFP-N3 vector. All transformants were maintained in the culture media without G418.

Western blotting analysis

The western blotting analysis was carried out according to previous reports (Miyazaki *et al.*, 2019; Kishimoto *et al.*, 2022). Briefly, the cultured cells were collected from the cell culture dishes by using

Molecular Pharmacology Fast Forward. Published on December 5, 2022 as DOI: 10.1124/molpharm.122.000597
This article has not been copyedited and formatted. The final version may differ from this version.

cell scrapers after washed with phosphate-buffered saline (PBS), and then cells were centrifuged at 3,500 g for 5 min at 4°C. The cell pellet was homogenized by sonication after being lysed with RIPA buffer (Nacalai Tesque, Inc., Kyoto, Japan), and then mixed with an equal amount of Laemmli sample buffer (Sigma-Aldrich). Protein samples (30 μg/well) were separated by SDS-polyacrylamide gel electrophoresis and transferred to a nitrocellulose membrane. The membranes were probed with the MUC1 [anti-MUC1 mouse monoclonal antibody (VU4H5); Santa Cruz Biotechnology Cat# sc-7313], MUC13 (anti-MUC13 rabbit polyclonal antibody; Thermo Fisher Scientific Cat# PA5-23249), P-gp [anti-P-glycoprotein mouse monoclonal antibody (C219); Millipore Cat# 517310-500UL], and β-actin (anti-β-actin mouse polyclonal antibody; Santa Cruz Biotechnology Cat# sc-47778) primary antibodies at a dilution of 1:1,000 overnight at 4°C. After washing three times with Tris-buffered saline (pH 7.4) containing 0.01% Tween 20, the membrane was incubated with anti-rabbit (HRP-linked whole Ab donkey; GE Healthcare Cat# GENA934,) or anti-mouse IgG (HRP-linked whole Ab sheep; GE Healthcare Cat# NA931) secondary antibodies at a dilution of 1:5,000 for 1 hour at room temperature. The protein bands were determined by enhanced chemiluminescence using the ECL Prime western blotting detection reagent (GE Healthcare) and their intensity was determined by the LAS-3000 system (Fuji Film, Tokyo, Japan).

Immunofluorescence staining

The cellular localization of mucin proteins was visualized with antibodies and lectins. Briefly, cells were washed twice with PBS and then fixed with 4% paraformaldehyde in PBS for 15 min. After washing twice with PBS, the cells were blocked with 10% bovine serum albumin (BSA) in PBS at 37°C for 30 min, and then incubated with the MUC1 antibody, MUC13 antibody, biotin-conjugated peanut agglutinin (PNA; Vector Laboratories Cat# B-1075), or biotin-conjugated Ulex europaeus agglutinin I (UEA I; Vector Laboratories Cat# B-1065) at a dilution of 1:200 for 2 hours at 37°C. After washing twice, the cells were stained using Alexa fluor 594-conjugate secondary antibody (1:1000) or Alexa Fluor 594-conjugate streptavidin (1:1000) at 37°C for 60 min. The cells were washed twice, then stained nuclei with Hoechst 33342, and visualized using a BZ-X710 microscope (KEYENCE,

Molecular Pharmacology Fast Forward. Published on December 5, 2022 as DOI: 10.1124/molpharm.122.000597
This article has not been copyedited and formatted. The final version may differ from this version.

Osaka, Japan). In addition, the subcellular localization of EGFP-tagged proteins was directly observed by BZ-X710.

Cytotoxic assay

Cytotoxicity was assessed using the MTT Cell Growth Assay Kit (Merck Millipore). MCF7 cells were incubated in the normal culture medium for 24 hours, then exposed to various concentrations of drugs for 72 hours. All stock solutions of the drugs were prepared in DMSO and diluted into the normal culture medium at concentrations less than 0.5%. From the average data of concentration-response curves obtained from cytotoxic assay, the IC_{50} values were obtained using the concentration-response stimulation non-linear regression model by GraphPad Prism v9.2 software (San Diego, CA).

Uptake study

The uptake study was conducted according to previous reports (Higuchi *et al.*, 2022; Tomabechi *et al.*, 2022). Stably transfected MCF7 cells were seeded at a density of 2×10^5 cells on a collagen-coated (collagen I, rat tail; Thermo Fisher Scientific, Inc., Waltham, MA) 24-well plate and cultured overnight. The cells were equilibrated in a transport buffer [Hanks' balanced salt solution (HBSS) with 10 mM HEPES, pH 7.4]. The uptake was initiated by the supplementation of a transport buffer containing the test compounds. After incubation for the indicated time, the uptake was immediately terminated by the addition of an ice-cold transport buffer. Following the aspiration of the extracellular solution, cells were washed three times with ice-cold transport buffer. Intracellular PAC and rose bengal were extracted using the mobile phase solution (50% methanol containing 0.1% formic acid) and 0.3 M NaOH solution containing 0.1% TritonX-100, respectively. The uptake amounts quantified by LC-MSMS were normalized to cellular protein contents, which were measured using a TaKaRa Bradford protein assay kit (Takara Bio Inc.).

The cellular uptake of Hoechst 33342 was measured by flow cytometry. Briefly, stably transfected cells were cultured on 12-well plates overnight (3.0×10^5 cells/well). The cells were detached from

Molecular Pharmacology Fast Forward. Published on December 5, 2022 as DOI: 10.1124/molpharm.122.000597
This article has not been copyedited and formatted. The final version may differ from this version.

plates in PBS with EDTA (1 mM) and then centrifuged at 400 g for 5 min. The cells were equilibrated in 200 μL of transport buffer for 10 min after washing with the buffer. An equal volume of Hoechst 33342 solution (with a final concentration of 0.5–20 μM) in transport buffer was added to the cell suspension. After incubation for the indicated time, the cell suspension was mixed with ice-cold buffer to terminate the uptake. Subsequently, 1.0×10^4 cells were analyzed with a FACSCelesta (BD Biosciences, San Diego, CA) to measure the fluorescence intensity of Hoechst 33342. The mean fluorescence intensity was calculated by subtraction of the mean value of untreated cells with Hoechst 33342.

Analytical methods

The PAC concentration in the samples was analyzed using a Waters Acquity UPLC™ H-Class-Xevo TQD system (Waters, Manchester, UK). PAC were separated on an octadecylsilyl (ODS) column (Acquity UPLC™ BEH C18 column, 100 mm × 2.1 mm, particle size 1.7 μm; Waters), maintained at 35°C. The mobile phase solvent A consisted of 0.1% formic acid in water, and the mobile phase solvent B consisted of methanol. The flow rate of the mobile phases was kept at 0.2 mL/min. The initial mobile phase composition was 95% solvent A and 5% solvent B for 1.0 min. Between 1.0–2.0 min, solvent A was reduced linearly from 95 to 5%. These settings were maintained for 6.0 min. Between 6.0–6.5 min, solvent A was increased to 95.0%. The overall run time was 7.0 min. The electrospray ionization was operated in the positive mode. The parameters were set as follows: desolvation gas flow, 1000 L/h; cone gas flow, 50 L/h; capillary voltage, 3.0 kV; desolvation temperature, 500°C; source temperature, 120°C. The cone and collision voltages were set at 58 and 34 V, respectively. The MRM m/z transitions monitored were 876.5 to 308.1. The UPLC system and the mass spectrometer were controlled using the Mass Lynx software version 4.1 (Waters).

The rose bengal concentration was determined using a microplate reader at the absorbance wavelength of 474 nm.

Molecular Pharmacology Fast Forward. Published on December 5, 2022 as DOI: 10.1124/molpharm.122.000597
This article has not been copyedited and formatted. The final version may differ from this version.

Measurement of cell-associated water

The measurement of cell-associated water volume was carried out as described previously by Clegg *et al.* (Clegg and Jackson, 1988). Briefly, the cultured cells were isolated from the cell culture dishes by 1 mM EDTA-containing PBS treatment and then centrifuged at 400 g for 5 min. The cell pellet was suspended in 400 μL of PBS containing FD-4 (0.1%), a membrane-impermeable fluorescent probe, and incubated for 30 min at 4°C. The cell suspensions were overlayed on 15% cyclohexane (Tokyo Chemical Industry Co., Ltd.) in 1 mL of silicon oil (SH-550; Nacalai Tesque, Inc., Tokyo, Japan), then centrifuged at 3,500 g for 2.5 min. The aqueous phase was aspirated to remove FD-4 not associated with the cell pellet. The cell pellet was dissolved in 0.1 M NaOH, then neutralized with HCl. The concentration of FD-4 was determined using a fluorescence microplate reader at the excitation/emission wavelengths of 492/515 nm, and normalized by cellular protein content. The extracellular water volume adhering to the plasma membrane was calculated by using the initial FD-4 concentration.

Statistical analysis

All experiments were performed in duplicates or triplicates and repeated at least three independent experiments on different days. The data were expressed as the mean ± standard deviation (S.D.). The statistical significance was determined by either one-way ANOVA followed by Dunnett's test for multiple groups or unpaired t-test for two groups, to compare the values obtained from the cell line stably expressing MUC1 or MUC1ΔCT with those in mock cells. For all statistical analyses were performed on the basis of biological replicates with GraphPad Prism v9.2, and $p < 0.05$ was considered statistically significant. Calculated p-values should be interpreted as descriptive and not as hypothesis-testing. The experiments were designed to be exploratory and to test the biological hypotheses about the role of membrane-bound NG-MUC1 in cytotoxicity and the membrane permeation of anticancer drugs. As this study is exploratory, sample sizes were not pre-determined and chosen to verify the reproducibility of the data. Neither blinding, nor randomization was employed.

Molecular Pharmacology Fast Forward. Published on December 5, 2022 as DOI: 10.1124/molpharm.122.000597
This article has not been copyedited and formatted. The final version may differ from this version.

Data Availability

The data generated in this study are available within the article and its supplementary data files.

RESULTS

Establishment of stable MCF-7 cells lines expressing MUC1ΔCT

Kalra *et al*. previously suggested a role of endogenous *O*-glycoproteins, such as MUC1, in 5-FU resistance (Kalra and Campbell, 2007, 2009). To test whether exogenous MUC1 confers 5-FU resistance, we transiently transfected MCF-7 cells with MUC1 and assessed the 5-FU cytotoxicity by MTT assay. The transient MUC1 expression resulted in an increase in cell survival in the presence of 5-FU (50 μM) compared with that of mock cells (Figure S1). This preliminary data suggested that MUC1 could be involved in the chemoresistance against several drugs, including 5-FU, although the details of the underlying mechanism remained unclear. To exclude the MUC1 function-related cell proliferation activity and examine the role of NG-MUC1 in chemoresistance, we generated stable MCF7 cell lines expressing MUC1ΔCT (a signaling-deficient form due to cytoplasmic tail deletion as shown in Figure 1a) fused with GFP (MUC1ΔCT cells), just as well as those expressing MUC1-GFP (MUC1 cells). The expressions and localization of MUC1-GFP and MUC1ΔCT-GFP in the stable cell lines were confirmed by western blotting (Figure 1b) and immunofluorescence staining (Figure 1c). The western blotting analysis revealed that the expression levels of MUC1-GFP and MUC1ΔCT-GFP were comparable in both cell lines and the endogenous MUC1 level was very low in the mock cells (Figure 1b). However, both cellular GFP signals were obscure at the plasma membrane and showed different localization patterns (Figure 1c). MUC1-GFP was likely accumulated in the intracellular organelles, while MUC1ΔCT-GFP was diffusively distributed within the cells. To assess the surface expression of MUC1 and MUC1ΔCT, we attempted to visualize the NG-MUC1 at the cellular surface with the MUC1 antibody specific for the tandem repeat region of NG-MUC1 and glycan-binding receptors (lectins) (Figure 1c). The MUC1 antibody was strongly bound to both MUC1 and MUC1ΔCT cells, indicating the remarkable expressions of NG-MUC1 protein. Furthermore, PNA and

Molecular Pharmacology Fast Forward. Published on December 5, 2022 as DOI: 10.1124/molpharm.122.000597
This article has not been copyedited and formatted. The final version may differ from this version.

UEA I, which bind to *O*-linked *N*-acetylgalactosamine (GalNAc) and terminal α1,2-linked fucose residues in glycans, respectively (Taylor-Papadimitriou *et al.*, 1999; Saeland *et al.*, 2012), strongly stained the cellular surface of MUC1 and MUC1ΔCT cells. The signal intensities of PNA and UEA I in MUC1ΔCT cells were likely to be greater than those in MUC1ΔCT cells. These results indicate that MUC1 and MUC1ΔCT cells express highly glycosylated NG-MUC1at the plasma membranes. We thus decided to use MUC1ΔCT cells as a model that could exclusively reflect the functional characteristics of membrane-bound NG-MUC1 for subsequent drug transport and toxicity studies.

NG-MUC1 expression conferred drug resistance

To characterize how NG-MUC1 could potentially affect anticancer drug-related cytotoxicity, we carried out a cell survival assay using MUC1ΔCT and mock cells treated with different doses of 5-FU (0.5 pM–500 μM), CDDP (0.1 nM–2 mM), DOX (0.1–200 μM), and PAC (0.01 pM–2 mM) for 72 hours. We observed dose-dependent inhibitions in both cell types treated with individual anticancer drugs, although the inhibition patterns differed. Compared to the mock cells, the cell survival rates against the tested anticancer drugs exhibited an overall increase in MUC1ΔCT cells. In the case of 5-FU, the MUC1ΔCT cell survival increased within the concentration range over 100 nM compared with that in mock cells (Figure 2a), supporting the preliminary study showing 5-FU resistance in cells transiently-expressing MUC1 (Figure S1). Similar increases in cell survival were observed in CDDP-, DOX-, and PAC-treated MUC1ΔCT cells within rages between 50–200 (Figure 2d), 0.1–50 (Figure 2gc), and 0.01–200 μM (Figure 2j), respectively, although the survival curve was strikingly altered in DOX-treated MUC1ΔCT cells. Comparable alterations in chemoresistance was also observed in MUC1 cells (Figures 2b, e, h, and k), indicating that anti-apoptotic pathways mediated by MUC1-CT may contribute minimally to the chemoresistance. These results suggest that NG-MUC1 is exclusively involved in the acquisition of chemoresistance.

To quantitatively evaluate how NG-MUC1 affect anticancer drug cytotoxicity, we estimated the IC_{50} values from the corresponding anticancer drug concentration-response curves and compared them

Molecular Pharmacology Fast Forward. Published on December 5, 2022 as DOI: 10.1124/molpharm.122.000597
This article has not been copyedited and formatted. The final version may differ from this version.

(Table 1). As expected, the IC_{50} values for tested drugs were higher in MUC1ΔCT cells than in mock cells. The MUC1ΔCT-to-mock cell IC_{50} ratios resulted in one to three orders of magnitude-large values as follows in descending order: PAC (149-fold) > DOX (18.1-fold) > 5-FU (7.40-fold) > CDDP (2.99-fold), indicating the notable PAC resistance increase in the MUC1ΔCT cells.

To examine whether another mucin could induce drug resistance, we carried out the cytotoxic tests in cells stably expressing MUC13 fused with GFP (MUC13 cells). MUC13, a smaller membrane-bound mucin, is expressed highly in the healthy human intestine and is involved in the formation of extracellular glycocalyx in the intestinal epithelium (Maher *et al.*, 2011). Similar to other mucins, MUC13 has an *N*-terminal glycosylated extracellular domain. However, the extracellular domain size is relatively smaller than that of MUC1 (Chauhan *et al.*, 2009). As shown in Figure 2, however, we failed to observe the similar effect in MUC13 cells as the cell survival curves for the individually tested drugs were almost the same between the MUC13 cells and mock cells. The surface expression of MUC13 was confirmed by immunofluorescence staining, but the PNA binding was weaker than those observed in MUC1 and MUC1ΔCT cells (Figures S2b, c). Given that the amino acid sequence of extracellular MUC13 domain is approximately one-third that of MUC1 and exhibits fewer *O*-glycosylation sites compared to that in MUC1 (Figure S4a), the molecular size in *O*-glycoprotein might be one of important factors in NG-MUC1-mediated chemoresistance.

NG-MUC1 expression reduced PAC uptake

To investigate whether the drug resistance involves alteration of drug permeability and accumulation, we performed a PAC uptake study in MUC1ΔCT, MUC1, MUC13, and mock cells (Figure 3a). The PAC uptake in the MUC1ΔCT cells significantly decreased to 51% compared to mock cells. The MUC1 cells were also tested, and the PAC uptake significantly decreased to 47%. In contrast, such a decrease could not be observed in MUC13 cells. Since the efflux transporters are major factors in modulating cellular drug uptake (Gottesman and Pastan, 1993), we verified the expression of P-glycoprotein (P-gp) involved in PAC efflux through western blotting (Figure S3) on cell lysates

Molecular Pharmacology Fast Forward. Published on December 5, 2022 as DOI: 10.1124/molpharm.122.000597
This article has not been copyedited and formatted. The final version may differ from this version.

from these cell lines. P-gp was expressed at a non-detectable level in MUC1ΔCT, MUC1, MUC13 and mock cells, while P-gp expression was detected in the positive control, Caco-2 cell lines, which are well known to express P-gp. These results indicate that P-gp is not involved in the reduced PAC uptake in MUC1ΔCT and MUC1 cells, and suggest that NG-MUC1 modulates the passive diffusion of PAC through the plasma membrane.

NG-MUC1 expression reduced intracellular Hoechst 33342 staining

To further verify the alteration of drug permeation and accumulation mediated by NG-MUC1 expression, we performed uptake studies through the nuclear staining with Hoechst 33342, which is a highly membrane-permeable cationic dye that emits blue fluorescence when bound to DNA (Figures 3b, c). The monitoring of fluorescence intensity in the uptake studies allows to assess whether the intracellular level of Hoechst 33342 is altered in MUC1ΔCT mock cells, because cell-adherent Hoechst 33342 emit no fluorescence. The flow cytometry analysis revealed that the Hoechst 33342 nuclear staining decreased in MUC1ΔCT and MUC1 cells compared to mock cells (Figure 3b), indicating a lower intracellular level of Hoechst 33342 in MUC1ΔCT cells. Furthermore, the decrease of Hoechst 33342 staining was greater in low concentrations (0.5–5 μM) than higher condition (10, 20 μM) (Figure 3c), suggesting the limitation in membrane permeation of Hoechst 33342 in MUC1ΔCT cells. Similar results were obtained in MUC1 cells (Figure 3c). To examine the contribution of electric charge state in permeates, we performed uptake studies using rose bengal, a cell-permeable anionic dye (Figure S4). The cell-associated staining in MUC1ΔCT and MUC1 cells significantly decreased to 67 and 38%, respectively, compared to mock cells. Therefore, there results suggest that NG-MUC1 is involved in the regulation to the passive diffusion regardless of the charge states of permeants.

NG-MUC1 expression increased the cell-adhered water volume

We attempted to evaluate the NG-MUC1 surface expression-related hydrophilic characteristics of the MUC1 and MUC1ΔCT cells by measuring the volume of cell-adhering water. It was found that the cell-adhered water volume was greater in MUC1ΔCT and MUC1 cells than mock cells, indicating that

Molecular Pharmacology Fast Forward. Published on December 5, 2022 as DOI: 10.1124/molpharm.122.000597
This article has not been copyedited and formatted. The final version may differ from this version.

NG-MUC1 could alter the cellular phenotype in physicochemical properties (Figures 3d).

NG-MUC1 expression confers anticancer drug resistance and limits the drug permeation

To further demonstrate the role of NG-MUC1 in chemoresistance, we generated stable cell lines of HeLa (cervical cancer cell line), A549 (lung cancer cell line), and HEK293 cells (embryonic kidney immortalized cell line) expressing GFP-fused MUC1ΔCT, and examined the membrane permeability and anticancer drug cytotoxicity (Figure 4). We found that remarkable expression of cell surface NG-MUC1 and glycans in all MUC1ΔCT cell types. NG-MUC1 expression resulted in significant increases ($p < 0.0001$) in cell survival in the presence of PAC compared to mock cells (Figure 4a–c, g). Furthermore, the Hoechst 33342 nuclear staining significantly decreased in all MUC1ΔCT cell types compared to mock cells (Figure 4d–f). These data indicate that MUC1ΔCT conferred anticancer drug resistance regardless of cancer cell type or cancer origin, and that NG-MUC1 is involved in the regulation of drug permeation across the plasma membrane.

DISCUSSION

The critical role of MUC1 in cancer has been already well-established; however, the impacts on the drug resistance have not yet been fully elucidated. In this study, we demonstrated that the extracellular MUC1 domain (NG-MUC1) is involved in drug resistance by limiting drug permeation across the plasma membrane. To the best of our knowledge, it is the first report on drug permeation and accumulation being affected by the expression of an *O*-glycoprotein, especially the membrane-bound-type mucin, MUC1, in mammalian cells.

Our findings that the membrane-bound NG-MUC1 expression in the form of MUC1ΔCT conferred anticancer drug resistance in MCF-7 cells support the hypothesis that MUC1 functions as a barrier element, protecting the cells from chemical exposure (Kufe, 2009; Jonckheere *et al.*, 2014; Leal *et al.*, 2017). Although MUC1 is known as an important factor in cancer chemoresistance, multiple studies

Molecular Pharmacology Fast Forward. Published on December 5, 2022 as DOI: 10.1124/molpharm.122.000597
This article has not been copyedited and formatted. The final version may differ from this version.

have focused on elucidating the molecular mechanism involved in transcriptional regulation (Ren *et al.*, 2006; Kufe, 2012; Nath *et al.*, 2013). Indeed, MUC1-CT, the cytoplasmic tail of MUC1, is a unique domain that interacts with various proteins involved in transcriptional regulation, thereby leading to the activation of antiapoptotic and proliferative signaling pathways (Ren *et al.*, 2004; Wei *et al.*, 2007; Yin *et al.*, 2010). However, we demonstrated that MUC1 confers chemoresistance without MUC1-CT (Figure 2, 4). Therefore, MUC1 exhibits dual functions in chemoresistance. In particular, the intact form of MUC1 expressed at the plasma membrane might be involved in NG-MUC1- rather than MUC1-CT-based chemoresistance, considering that MUC1-CT signaling must be accompanied by MUC1 decomposition (followed by the release of MUC1-CT).

NG-MUC1-mediated chemoresistance was associated with the alteration of drug permeability in the plasma membrane. We demonstrated that the NG-MUC1 expressions reduced the membrane permeability of several compounds including anticancer drug (Figures 3, S4), convincingly accounting for the observed chemoresistance. Although P-gp is a well-known efflux pump mediating the active transport of anticancer drugs, its involvement or contribution to chemoresistance was negligible in our study (Figure S3). However, it is well known that efflux transporters are involved in the drug resistance of many anticancer drugs (Tyner *et al.*, 2022). Thus, it should be necessary to carefully evaluate the contribution of transporters including BCRP and MRPs when considering the effects of NG-MUC1 on a wide range of drugs. Taken together, these data indicate that the extracellular domain of the membrane-bound MUC1 alters the passive diffusion-related plasma membrane properties.

Although the molecular mechanism of how the membrane-bound MUC1 affects membrane permeation remains unsolved, our results showing the remarkable paclitaxel IC_{50} alteration in MUC1ΔCT cells (Figure 2 and Table 1) could provide a clue to further unravel the underlying mechanisms. Indeed, the concentration-response curves shifted almost in parallel, but in some cases changed shapes (Figure 2), suggesting that several factors may regulate the effect of NG-MUC1 on limiting the membrane permeation of drugs. It has been proposed that MUC1 acts as a physical barrier

Molecular Pharmacology Fast Forward. Published on December 5, 2022 as DOI: 10.1124/molpharm.122.000597
This article has not been copyedited and formatted. The final version may differ from this version.

by meditating two functions (Jonckheere *et al.*, 2014). First, acting as a "molecular sieve" to limit the size of drug permeability through an intermolecular network. Second, acting as an "electrostatic capture" for the positively charged molecules based on the electrochemical property of the acidic MUC1 *O*-glycoprotein. Certainly, PAC is a chemical compound with a relatively high molecular weight (853.9 Da) but this size is markedly smaller than several peptides including EGF (epidermal growth factor; 6045 Da), which must contact with the cell surface physiologically. In terms of molecular size, the molecular sieve may hardly distinguish PAC from 5-FU (130.1 Da), with an IC_{50} solely changed to some extent in MUC1ΔCT cells, since globular proteins (15–650 kDa) including albumin, can diffuse freely through the mucus (Olmsted *et al.*, 2001). Therefore, molecular size is unlikely to be a major factor in our observation. Furthermore, the electrostatic interaction is also an unlikely possibility as PAC is rather highly lipophilic (log *P* = 3.54) than hydrophilic. As the alteration of the PAC membrane permeation in MUC1ΔCT cells cannot be simply explained by previously proposed processes.

It is noteworthy that the cell-adhered water volume increase in the MUC1ΔCT and MUC1 cells indicates that NG-MUC1 could alter the cellular phenotype in physicochemical properties (Figure 3d). A recent study showed that the deglycosylation of a mucus extract resulted in dehydration and loss of lubrication capacity (Crouzier *et al.*, 2015). Sadzuka *et al*. reported that the surface modification of liposomes with polyethylene glycols increased the apparent thickness of the aqueous layer on the liposomes depending on the molecular weight and size (Sadzuka *et al.*, 2002). Therefore, the observed water volume increase seems to depend on the degree of glycosylation in the cells. We speculate that the extracellular domain of membrane-bound MUC1 constitutes the water layer on the cell surface and suggest that the water layer is involved in the modification of the membrane permeation in the cells. Indeed, the thickness of the water layer in the MUC1ΔCT and MUC1 cells was estimated to be 17.0 ± 7.7 and 16.4 ± 5.5 nm/cell, respectively (based on the data in Figure 3 and the cell volume with an assumption of a spherical cell, calculated by the following equation: $V = 4/3 \times \pi r^3$, where r is the cell radius), and significantly larger than that in the mock cells (9.3 ± 5.3 nm/cell). In MUC13 cells, where

Molecular Pharmacology Fast Forward. Published on December 5, 2022 as DOI: 10.1124/molpharm.122.000597
This article has not been copyedited and formatted. The final version may differ from this version.

no chemoresitance was observed, the putative water layer thickness (11.0 ± 5.2 nm/cell) is comparable to the mock cells. Considering our findings that MUC1ΔCT and MUC1, but not MUC13, altered chemoresistance, the water layer thickness might be related to the drug membrane permeation.

Given that the unstirred water layer (UWL) adjacent to the intestinal brush border membrane limits the apparent lipophilic compound permeability (Ho and Higuchi, 1974), the NG-MUC1-related putative water layer might reduce lipophilic anticancer drug membrane permeability, especially that of PAC. Assuming restricted aqueous diffusion via NG-MUC1 at the cell surface, the cell-adhered water might show similar characteristics in the UWL layer. Thus, the idea that NG-MUC1 creates a water layer similar to UWL may explain our results that the degree of drug resistance varied among drugs and likely depended on their lipophilicity. Typical mucus secretions, composed of secretory-type mucins, reportedly exhibit nearly 100–1,000 times higher viscosity than that of water (Lai *et al.*, 2009), suggesting the lack of water stirring in the mucus networks. Such “bound water” in polymer compounds has been considered to have different properties from bulk water (J Hoeve and Kaklvaya, 2002; Jahn and Klein, 2015). However, the characteristics of bound water in the membrane permeability of drugs have not yet been defined. Therefore, further studies would be required to elucidate such a relationship.

In conclusion, we clarified the role of MUC1 as a hydrophilic barrier element against anticancer drugs and the importance of NG-MUC1 in the reduction of membrane permeation. We suggest the involvement of the NG-MUC1-created cell surface water layer in the membrane permeation of lipophilic drugs. Our findings could help better understanding the molecular basis of drug resistance in cancer chemotherapy.

AKNOWLEDGEMETNS

We are grateful to Dr. Akinori Hisatsune for generously providing us MUC1/pcDNA3.1(+).

Molecular Pharmacology Fast Forward. Published on December 5, 2022 as DOI: 10.1124/molpharm.122.000597
This article has not been copyedited and formatted. The final version may differ from this version.

AUTHOR CONTRIBUTIONS

Participated in research design: Miyazaki, Kishimoto, and Inoue.

Conducted experiments: Miyazaki, Kishimoto, Kobayashi, and Suzuki.

Performed data analysis: Miyazaki, Kishimoto, Kobayashi, Suzuki, Higuchi, Shirasaka, and Inoue.

Wrote or contributed to the writing of the manuscript: Miyazaki, Kishimoto, and Inoue.

Molecular Pharmacology Fast Forward. Published on December 5, 2022 as DOI: 10.1124/molpharm.122.000597
This article has not been copyedited and formatted. The final version may differ from this version.

REFERENCES

Adashek JJ, Desai AP, Andreev-Drakhlin AY, Roszik J, Cote GJ, Subbiah V (2021) Hallmarks of RET and co-occuring genomic alterations in RET-aberrant cancers. *Mol Cancer Ther* **20**: 1769–1776.

Carson DD (2008) The cytoplasmic tail of MUC1: A very busy place. *Sci Signal* **1**: pe35

Chauhan SC, Vannatta K, Ebeling MC, Vinayek N, Watanabe A, Pandey KK, Bell MC, Koch MD, Aburatani H, Lio Y, and Jaggi M (2009) Expression and functions of transmembrane mucin MUC13 in ovarian cancer. *Cancer Res* **69**: 765–774.

Clegg JS, and Jackson SA (1988) Glycolysis in permeabilized L-929 cells. *Biochem J* **255**: 335–344.

Crouzier Thomas, Boettcher Kathrin, Geonnotti Anthony R, Kavanaugh Nicole L, Hirsch Julie B, Ribbeck Katharina, Lieleg Oliver, Crouzier T, Kavanaugh N L, Ribbeck K, Boettcher K, Lieleg O, Geonnotti A R, and Hirsch J B (2015) Modulating mucin hydration and lubrication by deglycosylation and polyethylene glycol binding. *Adv Mater Interfaces* **2**: 1500308.

Furuta T, Ueda T, Aune G, Sarasin A, Kraemer KH, and Pommier Y (2002) Transcription-coupled nucleotide excision repair as a determinant of cisplatin sensitivity of human cells. *Cancer Res* **62**: 4899–4902.

Gottesman MM, and Pastan I (1993) Biochemistry of multidrug resistance mediated by the multidrug transporter. *Annu Rev Biochem* **62**: 385–427.

Hata T, Rajabi H, Takahashi H, Yasumizu Y, Li W, Jin C, Long MD, Hu Q, Liu S, Fushimi A, Yamashita N, Kui L, Hong D, Yamamoto M, Miyo M, Hiraki M, Maeda T, Suzuki Y, Samur MK, and Kufe D (2019) MUC1-C Activates the NuRD complex to drive dedifferentiation of triple-negative breast cancer cells. *Cancer Res* **79**: 5711–5722.

Higuchi K, Sugiyama K, Tomabechi R, Kishimoto H, and Inoue K (2022) Mammalian monocarboxylate transporter 7 (MCT7/Slc16a6) is a novel facilitative taurine transporter. *J Biol Chem* **298**: 101800.

Hisatsune A, Kawasaki M, Nakayama H, Mikami Y, Miyata T, Isohama Y, Katsuki H, and Kim KC. (2009) Internalization of MUC1 by anti-MUC1 antibody from cell membrane through the macropinocytotic pathway. *Biochem Biophys Res Commun* **388**: 677–682.

Ho NFH, and Higuchi WI (1974) Theoretical model studies of intestinal drug absorption IV: Bile acid transport at premicellar concentrations across diffusion layer-membrane barrier. *J Pharm Sci* **63**: 686–690.

Holohan C, van Schaeybroeck S, Longley DB, and Johnston PG (2013) Cancer drug resistance: an evolving paradigm. *Nat Rev Cancer* **13**: 714–726.

Hoeve CA, and Kaklvaya SR (1976) On the structure of water absorbed in collagen. *J Phys Chem* **80**: 745–749.

Jahn S, and Klein J (2015) Hydration lubrication: The macromolecular domain. *Macromolecules* **48**: 5059–5075.

Jonckheere N, Skrypek N, and van Seuningen I (2014) Mucins and tumor resistance to chemotherapeutic drugs. *Biochim Biophys Acta* **1846**: 142–151.

Kalra A V., and Campbell RB (2007) Mucin impedes cytotoxic effect of 5-FU against growth of human pancreatic cancer cells: overcoming cellular barriers for therapeutic gain. *Br J Cancer* **97**: 910–918.

Kalra A V., and Campbell RB (2009) Mucin overexpression limits the effectiveness of 5-FU by reducing intracellular drug uptake and antineoplastic drug effects in pancreatic tumours. *Eur J Cancer* **45**: 164–173.

Kishimoto H, Ridley C, and Thornton DJ (2022) The lipophilic cyclic peptide cyclosporin A induces aggregation of gel-forming mucins. *Sci Rep* **12**: 1–12.

Kobayashi S, Boggon TJ, Dayaram T, Jänne PA, Kocher O, Meyerson M, Johnson BE, Eck MJ, Tenen DG, and Halmos B (2009) EGFR mutation and resistance of non-small-cell lung cancer to gefitinib. *N Engl J Med* **352**: 786–792.

Kufe DW (2012) MUC1-C oncoprotein as a target in breast cancer: activation of signaling pathways and therapeutic approaches. *Oncogene* **32**: 1073–1081.

Kufe DW (2009) Mucins in cancer: function, prognosis and therapy. *Nat Rev Cancer* **9**: 874–885.

Lai SK, Wang YY, Wirtz D, and Hanes J (2009) Micro- and macrorheology of mucus. *Adv Drug Deliv Rev* **61**: 86–100.

Leal J, Smyth HDC, and Ghosh D (2017) Physicochemical properties of mucus and their impact on transmucosal drug delivery. *Int J Pharm* **532**: 555–572.

Leteurtre E, Gouyer V, Delacour D, Hémon B, Pons A, Richet C, Zanetta JP, and Huet G (2003) Induction of a storage phenotype and abnormal intracellular localization of apical glycoproteins are two independent responses to GalNAcα-O-bn. *J Histochem Cytochem* **51**: 349–361.

Levitin F, Stern O, Weiss M, Gil-Henn C, Ziv R, Prokocimer Z, Smorodinsky NI, Rubinstein DB, and Wreschner DH (2005) The MUC1 SEA module is a self-cleaving domain. *J Biol Chem* **280**: 33374–33386.

Linden SK, Sutton P, Karlsson NG, Korolik V, McGuckin MA. (2008) Mucins in the mucosal barrier to infection. *Mucosal Immunol* **1**: 183–197.

Maher DM, Gupta BK, Nagata S, Jaggi M, and Chauhan SC (2011) Mucin 13: Structure, function, and potential roles in cancer pathogenesis. *Mol Cancer Res* **9**: 531–537.

Meijer C, Mulder NH, Timmer-Bosscha H, Sluiter WJ, Meersma GJ, and de Vries EGE (1992) Relationship of cellular glutathione to the cytotoxicity and resistance of seven platinum compounds. *Cancer Res* **52**: 6885–6889.

Miyazaki K, Kishimoto H, Muratani M, Kobayashi H, Shirasaka Y, and Inoue K (2019) Mucins are involved in the intestinal permeation of lipophilic drugs in the proximal region of rat small intestine. *Pharm Res* **36**: 162.

Montero J, and Haq R (2022) Adapted to survive: Targeting cancer cells with BH3 mimetics. *Cancer Discov.* **12**: 1217–1232.

Nath S, Daneshvar K, Roy LD, Grover P, Kidiyoor A, Mosley L, Sahraei M, and Mukherjee P (2013) MUC1 induces drug resistance in pancreatic cancer cells via upregulation of multidrug resistance genes. *Oncogenesis* **2**: e51.

Olmsted SS, Padgett JL, Yudin AI, Whaley KJ, Moench TR, and Cone RA (2001) Diffusion of macromolecules and virus-like particles in human cervical mucus. *Biophys J* **81**:1930–1937.

Ren J, Agata N, Chen D, Li Y, Yu WH, Huang L, Raina D, Chen W, Kharbanda S, and Kufe D (2004) Human MUC1 carcinoma-associated protein confers resistance to genotoxic anticancer agents. *Cancer Cell* **5**: 163–175.

Ren J, Raina D, Chen W, Li G, Huang L, and Kufe D (2006) MUC1 oncoprotein functions in activation of fibroblast growth factor receptor signaling. *Mol Cancer Res* **4**: 73–883.

Sadzuka Y, Nakade A, Hirama R, Miyagishima A, Nozawa Y, Hirota S, and Sonobe T (2002) Effects of mixed polyethyleneglycol modification on fixed aqueous layer thickness and antitumor activity of doxorubicin containing liposome. *Int J Pharms* **238**: 171–180.

Saeland E, Belo AI, Mongera S, van Die I, Meijer GA, and van Kooyk Y (2012) Differential glycosylation of MUC1 and CEACAM5 between normal mucosa and tumour tissue of colon cancer patients. *Int J Cancer* **131**: 117–128.

Taylor-Papadimitriou J, Burchell J, Miles DW, and Dalziel M (1999) MUC1 and cancer. *Biochim Biophys Acta* **1455**: 301–313.

Tomabechi R, Kishimoto H, Sato T, Saito N, Kiyomiya K, Takada T, Higuchi K, Shirasaka Y, and Inoue K (2022) SLC46A3 is a lysosomal proton-coupled steroid conjugate and bile acid transporter involved in transport of active catabolites of T-DM1. *PNAS Nexus* **1**: pgac063

Tyner JW, Haderk F, Kumaraswamy A, Baughn LB, van Ness B, Liu S, Marathe H, Alumkal JJ, Bivona TG, Chan KS, Druker BJ, Hutson AD, Nelson PS, Sawyers CL, and Willey CD (2022) Understanding drug sensitivity and tackling resistance in cancer. *Cancer Res* **82**: 1448–1460.

Wang Z, Li Y, Ahmad A, Banerjee S, Azmi AS, Kong D, and Sarkar FH (2010) Pancreatic cancer: understanding and overcoming chemoresistance. *Nat Rev Gastroenterol Hepatol* **8**: 27–33.

Wei X, Xu H, and Kufe D (2007) Human mucin 1 oncoprotein represses transcription of the p53 tumor suppressor gene. *Cancer Res* **67**: 1853–1858.

Yin L, Ahmad R, Kosugi M, Kufe T, Vasir B, Avigan D, Kharbanda S, and Kufe D (2010) Survival of human multiple myeloma cells is dependent on MUC1 C-terminal transmembrane subunit oncoprotein function. *Mol Pharmacol* **78**: 166–174.

Zimmermann A, Zenke FT, Chiu LY, Dahmen H, Pehl U, Fuchss T, Grombacher T, Blume B, Vassilev LT, and Blaukat A (2022) A new class of selective ATM inhibitors as combination partners of DNA double-strand break inducing cancer therapies. *Mol Cancer Ther* **21**: 859–870.

Molecular Pharmacology Fast Forward. Published on December 5, 2022 as DOI: 10.1124/molpharm.122.000597
This article has not been copyedited and formatted. The final version may differ from this version.

FOOTNOTES

Financial support

This work was supported by research grants from Japan Research Foundation for Clinical Pharmacology [Grant Number 2018A06, H. Kishimoto] and JSPS KAKENHI [Grant Number 17K15522, H. Kishimoto].

COI

The authors declare no potential conflicts of interest.

Reprint requests

Katsuhisa Inoue

1432-1 Horinouchi, Hachioji, Tokyo 192-0392, Japan

E-mail: kinoue@toyaku.ac.jp

[1] These authors contributed equally to this work.

Molecular Pharmacology Fast Forward. Published on December 5, 2022 as DOI: 10.1124/molpharm.122.000597
This article has not been copyedited and formatted. The final version may differ from this version.

FIGURE LEGENDS

Figure 1. Construction of MUC1ΔCT-GFP stably-expressing cell lines (MUC1ΔCT cells). (a) Schematic representation of MUC1 and the truncated MUC1ΔCT constructs. Full-length MUC1-GFP and cytoplasmic tail (red box)-deleted MUC1ΔCT-GFP. (b) The expressions of MUC1-GFP and MUC1ΔCT-GFP in MCF7 cells were verified by western blotting. (c) The subcellular localization of MUC1-GFP and MUC1ΔCT-GFP were visualized by immunofluorescence staining using a MUC1 antibody and lectins. The nuclei were stained by Hoechst33342. The signals of GFP (green), anti-MUC1 (red), PNA (red), UEA I (red) and nuclei (blue) were observed by a fluorescence microscopy. Scale bars = 100 μm.

Figure 2. MUC1ΔCT confers resistance to various anticancer drugs. The cell viabilities were assessed by MTT assay using mock cells (open circle), MUC1ΔCT (closed triangle), MUC1 (closed circle), and MUC13 (closed square) treated with different concentrations of: (a–c) 5-FU (0.5 pM–500 μM); (d–f) cisplatin (0.1 nM–2 mM); (g–i) doxorubicin (0.1–200 μM); (j–l) paclitaxel (0.01 pM–2 mM) for 72 hours. Dotted line was referred to mock cells as control. Cell viability (measured as absorbance) is expressed as % untreated control. Results are presented as the mean ± S.D. from 6 independent experiments performed in triplicate. The solid curves were drawn by fitting the data to the three-parameter logistic equation by GraphPad Prism v9.2.

Figure 3. NG-MUC1 suppresses the intracellular accumulation of chemicals by the mechanism in which the cell-adhered water is involved. (a) The uptake experiment was performed with PAC (10 μM, 60 min). (b) Hoechst 33342 uptake (0.5 μM) were analyzed by FACS for 30 min. (c) Dose-dependent uptake of Hoechst 33342 (0.5–20 μM, for 15 min) were analyzed by FACS. (d) The cell-adhered water volume. The results are presented as the mean ± S.D. from 5 (mock), 8 (MUC1ΔCT), 3 (MUC1), and 3 (MUC13) independent experiments performed in triplicates, respectively (a), 4 independent experiments (b), 6 (0.5 and 1 μM), 4 (2.5 μM), and 3 (5–20 μM) independent experiments, respectively (c), and 5 (mock), 8 (MUC1ΔCT), 7 (MUC1), and 5 (MUC13) independent experiments

Molecular Pharmacology Fast Forward. Published on December 5, 2022 as DOI: 10.1124/molpharm.122.000597
This article has not been copyedited and formatted. The final version may differ from this version.

performed in triplicates, respectively (d). * $p < 0.05$, ** $p < 0.01$ compared with the control (mock cells).

Figure 4. MUC1ΔCT confers anticancer drug resistance and limits the membrane permeation and accumulation of intracellular Hoechst 33342 staining. (a–c) The cell viabilities were assessed using MUC1ΔCT and mock cells in 72 hours post-treatment of paclitaxel (HeLa; 1 μM, A549; 0.01 μM, HEK293; 10 μM) for 72 h. Cell viability (measured as absorbance) is expressed as % untreated control. (d–f) Hoechst 33342 uptake (0.5 μM, for 15 min) were analyzed by FACS. The results are presented as the mean ± S.D. from 5 independent experiments performed in duplicates (a–c), and 9 (HeLa), 6 (A549), and 9 (HEK293) independent experiments, respectively (d–f). * $p < 0.05$, ** $p < 0.01$ compared with the control (mock cells). (g) The cellular localization of MUC1ΔCT-GFP was visualized by immunofluorescence staining using MUC1 antibody and lectins. The nuclei were stained by Hoechst33342. GFP (green), anti-MUC1 (red), PNA (red), UEA I (red), and nuclei (blue) were observed by fluorescence microscopy. Scale bars = 100 μm.

Molecular Pharmacology Fast Forward. Published on December 5, 2022 as DOI: 10.1124/molpharm.122.000597
This article has not been copyedited and formatted. The final version may differ from this version.

Table 1. IC_{50} values for various anticancer drugs calculated from concentration-response curves

	IC_{50} (μM)		
	mock	MUC1ΔCT cells	MUC1 cells
5-FU	0.05	0.37 (7.40)	1.49 (29.8)
CDDP	28.81	86.16 (2.99)	259.26 (9.00)
DOX	0.24	4.34 (18.1)	4.61 (19.2)
PAC	0.28	41.81 (149)	186.68 (667)

The approximate IC_{50} values were calculated from the average of concentration-response curves in the MUC1ΔCT, MUC1, and mock cells treated with anticancer drugs (Figure 2). The values in parentheses show IC_{50} ratio relative to that in mock cells.

Molecular Pharmacology Fast Forward. Published on December 5, 2022 as DOI: 10.1124/molpharm.122.000597
This article has not been copyedited and formatted. The final version may differ from this version.

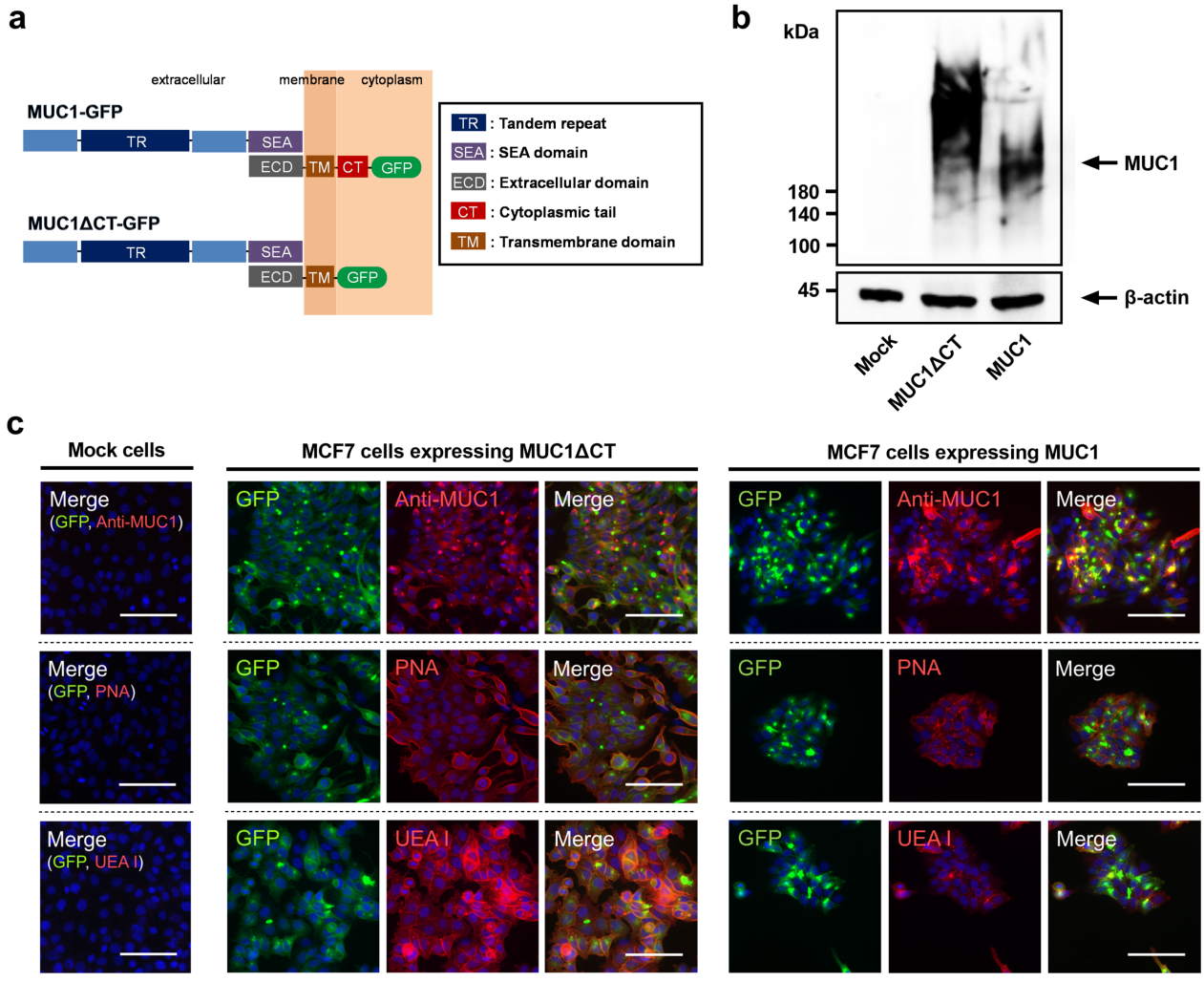

Figure 1

Molecular Pharmacology Fast Forward. Published on December 5, 2022 as DOI: 10.1124/molpharm.122.000597
This article has not been copyedited and formatted. The final version may differ from this version.

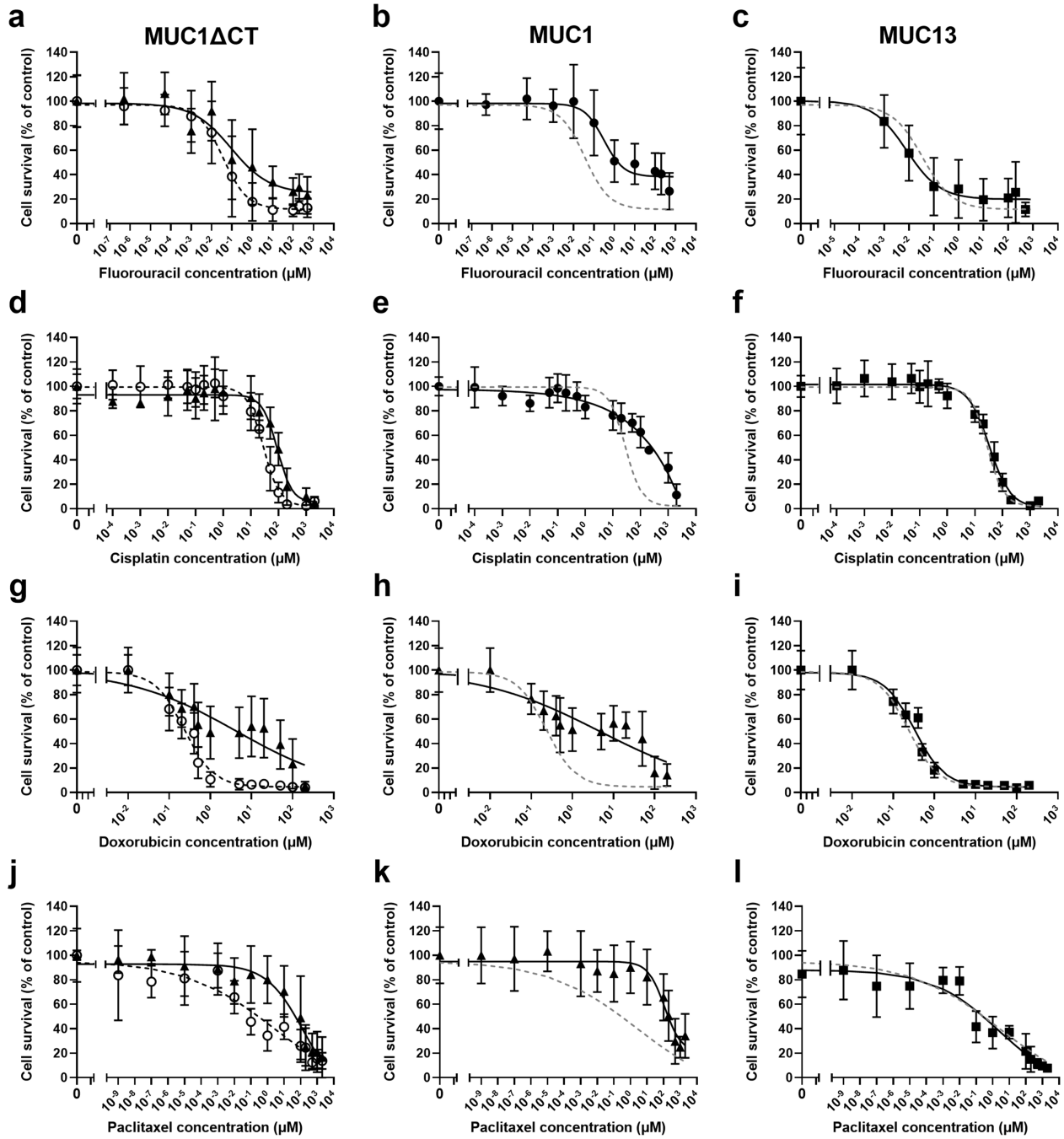

Figure 2

Molecular Pharmacology Fast Forward. Published on December 5, 2022 as DOI: 10.1124/molpharm.122.000597
This article has not been copyedited and formatted. The final version may differ from this version.

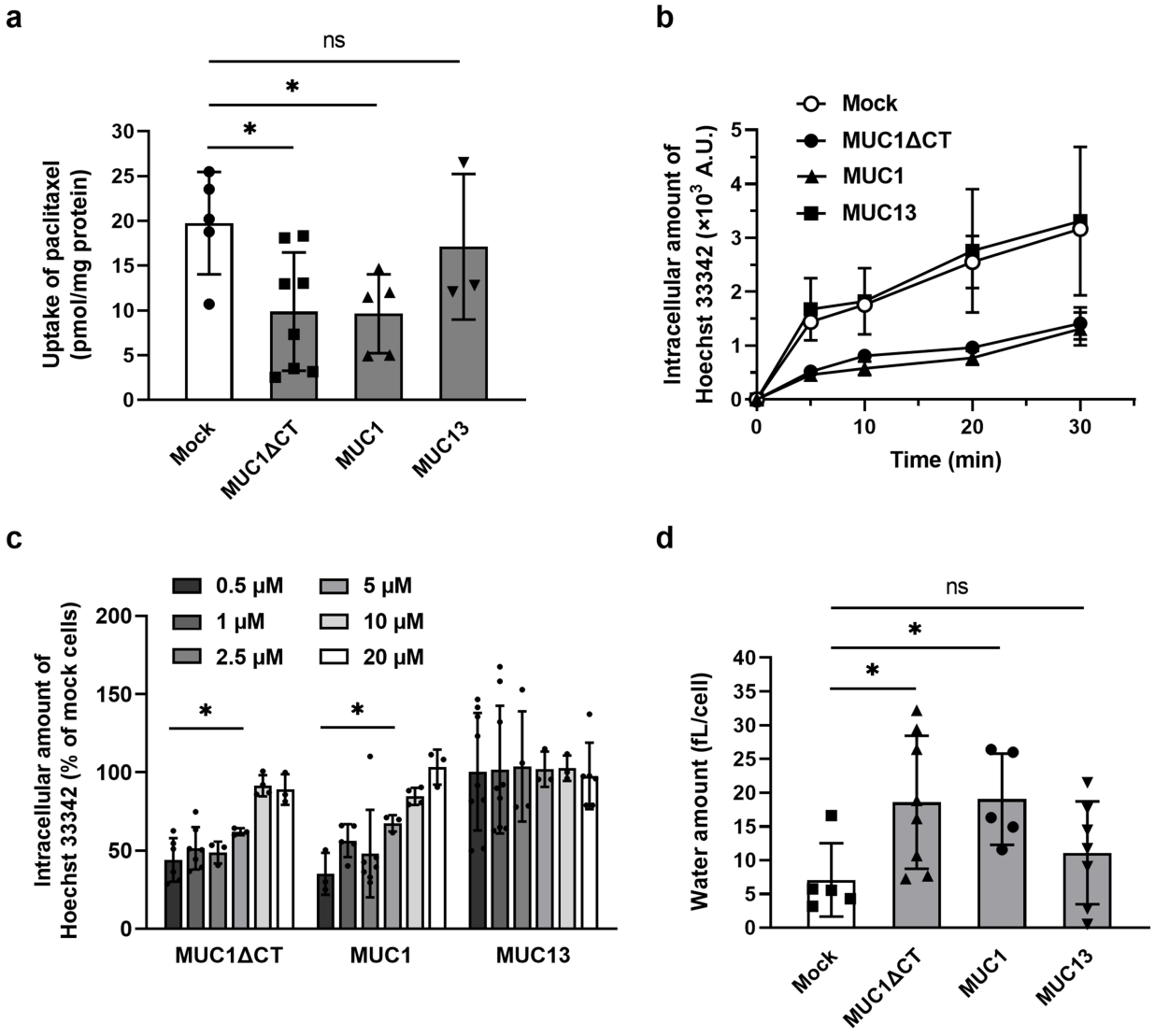

Figure 3

Molecular Pharmacology Fast Forward. Published on December 5, 2022 as DOI: 10.1124/molpharm.122.000597
This article has not been copyedited and formatted. The final version may differ from this version.

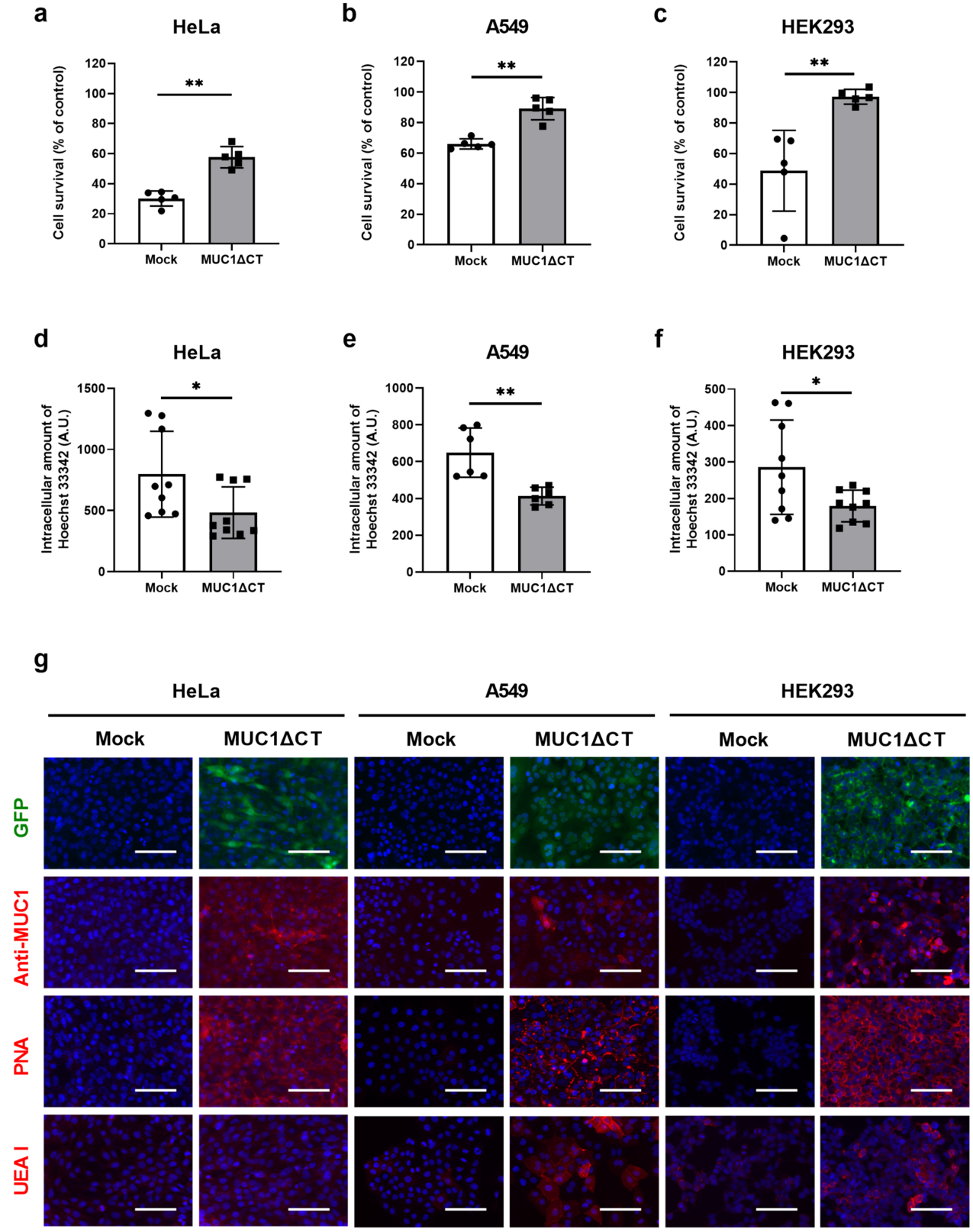

Figure 4